Neuronal polarity is regulated by a direct interaction between a scaffolding protein, Neurabin, and a presynaptic SAD-1 kinase in *Caenorhabditis elegans*

Wesley Hung, Christine Hwang, Michelle D. Po and Mei Zhen*

The establishment of axon-dendrite identity in developing neurites is essential for the development of a functional nervous system. The SAD serine-threonine kinases have been implicated in regulating neuronal polarization and synapse formation. Here, we show that the *C. elegans* SAD-1 kinase regulates axonal identity and synapse formation through distinct mechanisms. We identified a scaffolding protein, Neurabin (NAB-1), as a physiological binding partner of SAD-1. Both *sad-1* and *nab-1* loss-of-function mutants display polarity defects in which synaptic vesicles accumulate in both axons and dendrites. We show that *sad-1* and *nab-1* function in the same genetic pathway to restrict axonal fate. Unlike *sad-1*, *nab-1* mutants display normal morphology of vesicle clusters. Strikingly, although the physical interaction of NAB-1 with SAD-1 is necessary for polarity, it is dispensable for synapse morphology. We propose that Neurabin functions as a scaffold to facilitate SAD-1-mediated phosphorylation for substrates specific for restricting axonal fate during neuronal polarization.

KEY WORDS: sad-1, Neurabin, Neuronal polarity, *Caenorhabditis elegans*

INTRODUCTION

The development of a functional nervous system requires the maturation of neurons and the establishment of synaptic contacts between neurons and their target cells. Mature neurons are highly polarized cells with morphologically and functionally distinct axons and dendrites. The process of axon and dendrite specification, best observed and most extensively studied in isolated rat hippocampal neuron cultures, is divided into several stages (Dotti et al., 1988). Initially, multiple short and morphologically undifferentiated neurites develop from embryonic neurons. Then, a single neurite extends rapidly and acquires axonal characteristics, which is followed by the maturation of the remaining neurites as dendrites. The sequential axon and dendrite differentiation events are driven by multiple intrinsic mechanisms (reviewed in Arimura and Kaibuchi, 2005; Wiggin et al., 2005). The Par3-Par6-aPKC 'polarity' complex is recruited to the growing axon tip (Shi et al., 2003) where it activates the small GTPase Rac1 (Etienne-Manneville and Hall, 2001; Menager et al., 2004; Nishimura et al., 2005; Shi et al., 2003). Rac1-driven actin remodeling of cytoskeleton supports the fast extension of the neurite that is required for the specification of axonal fate (Nishimura et al., 2005). Interactions between Par3 and the Rac-specific guanine-exchange factor (GEF) Tiam1 further induce Rac1 activity (Chen and Macara, 2005; Nishimura et al., 2005).

Microtubule dynamics also regulate axon formation. Axons and dendrites display different microtubule organizations and are decorated with different microtubule-binding proteins (MAPs) (Baas et al., 1989). MAP1B and Tau are axon-enriched MAPs (Bouquet et al., 2004; Goold and Gordon-Weeks, 2005; Kempf et al., 1996). Their phosphorylation by kinases, including GSK3β,

Samuel Lunenfeld Research Institute, Mount Sinai Hospital and Department of Microbiology and Medical Genetics, University of Toronto, Ontario, M5G 1X5, Canada.

*Author for correspondence (e-mail: zhen@mshri.on.ca)

PAR-1, SAD-A (Brsk2) and SAD-B (Brsk1), reduces their association with microtubules and destabilizes microtubule assembly, which is a process that facilitates the initiation of axon outgrowth and specification (Biernat et al., 2002; Kishi et al., 2005; Trivedi et al., 2005).

Although primary neuronal cultures have been the most widely used system to study neuronal polarity, in vivo systems are essential for the elucidation and functional validation of neuronal-polarity regulators (Rolls and Doe, 2004). The fully elucidated neural-circuit diagrams (White et al., 1986) and the development of fluorescent markers for nerve processes in *C. elegans* allow for in vivo analysis of neuronal polarity. Neuronal polarity can be observed in both sensory and motor neurons using synaptic components, which are stereotypically restricted to specific regions of nerve processes, as markers to distinguish the axonal and dendritic processes. Recent studies have revealed that the wnt signaling pathway is required for anteriorly-directed axonal extension in mechanosensory neurons (Hilliard and Bargmann, 2006; Pan et al., 2006; Prasad and Clark, 2006). SYD-1, a putative Rho GTPase-activating protein, restricts presynaptic proteins to the axons of both motoneurons and chemosensory neurons (Hallam et al., 2002).

Loss-of-function mutations in the *C. elegans sad-1* gene, a member of the conserved SAD-family serine-threonine kinase, lead to axon-termination defects, diffuse synaptic-vesicle clustering and the abnormal accumulation of presynaptic proteins in the dendrites of the DD-class GABAergic motoneurons (Crump et al., 2001), suggesting that SAD-1 regulates both neuronal polarity and synapse formation. Morpholino-induced downregulation of the ascidian SAD-family kinase POPK-1 disrupts the proper translocation of maternal mRNAs in ascidian embryos (Nakamura et al., 2005). Double knockout mice of the two mammalian SAD kinases, SAD-A and SAD-B, fail to develop distinct axons and dendrites in cortical and hippocampal neurons, and they exhibit a reduced level of MAP Tau1 phosphorylation (Kishi et al., 2005), suggesting that they function redundantly to specify neurite identity. A recent report suggests that SAD-B associates with synaptic vesicles and active zones in mature synapses, and may also regulate synaptic

transmission (Inoue et al., 2006). The molecular pathways through which SAD kinases function to establish neuronal polarity and synapse formation remain unknown.

To identify genes that regulate or mediate the function of SAD-1, we performed a yeast two-hybrid screen and identified the sole *C. elegans* homolog of Neurabin (NAB-1) that physically interacts with SAD-1 both in vivo and in vitro. Mammalian Neurabin (NeurabinI) and Spinophilin (NeurabinII) were first isolated as F-actin-binding proteins from the rat brain (Allen et al., 1997; Nakanishi et al., 1997; Satoh et al., 1998). They are scaffolding proteins that interact with multiple partners, including protein phosphatase-1 (PP1), p70 S6 kinase, Rac3, the Rho-specific GEF Lfc and the Rac-specific GEF Tiam1 (Buchsbaum et al., 2003; Burnett et al., 1998; Orioli et al., 2006; Ryan et al., 2005; Terry-Lorenzo et al., 2002a; Terry-Lorenzo et al., 2002b). Spinophilin can also interact with G-protein coupled D2 dopamine receptors and α2 adrenergic receptors (Richman et al., 2001; Smith et al., 1999; Wang et al., 2005). In neurons, both Neurabin and Spinophilin are localized at synapses (Nakanishi et al., 1997), enriched and closely associated with the postsynaptic density in mature neurons (Muly et al., 2004a; Muly et al., 2004b), where they recruit PP1 and Lfc to dendritic spines and regulate their morphology and motility (Ryan et al., 2005; Terry-Lorenzo et al., 2005). The elimination of Neurabin expression by antisense-oligonucleotide blocks neurite formation in cultured neurons (Nakanishi et al., 1997), suggesting a role of Neurabin prior to dendritic-spine maturation. Spinophilin and Neurabin single knock-out mice are viable (Allen et al., 2006; Feng et al., 2000) and display altered dopamine-mediated synaptic plasticity; Neurabin and Spinophilin mutants are deficient in long-term potentiation and depression, respectively (Allen et al., 2006; Feng et al., 2000). The viability and mild phenotypes of either single knockout suggest a functional redundancy between these two proteins.

Through biochemical and genetic studies, we now demonstrate that *C. elegans* Neurabin plays an 'earlier' role in neurons, where it physically interacts with, and specifically mediates, the function of the SAD-1 kinase to restrict axonal fate in developing neurites.

MATERIALS AND METHODS
Strains
All strains were cultured at 22°C. *nab-1*-deletion mutants, *ok943* and *gk164* were backcrossed four times against wild-type strain N2 prior to phenotypic and biochemical analysis, and double- and triple-mutant construction.

Plasmids
The *nab-1* genomic clone pJH513 contains the 9 kb promoter sequence upstream of ATG, the entire gene and the 1 kb downstream sequence. The NAB-1::GFP clone pJH369 was generated from pJH513 by inserting GFP immediately before the stop codon. The *nab-1* mini-gene – which contains a cDNA fragment (encoding the first 378 amino acids) that was combined with a genomic fragment – including the last two introns, was inserted into the C-terminal of *Punc-25*-GFP and mRFP vectors to create pJH507 (*Punc-25* NAB-1::GFP) and pJH510 (*Punc-25* NAB-1::mRFP), respectively. pJH524 (*Pmyo-3* NAB-1::mRFP) was created by inserting the NAB-1::mRFP fragment from pJH510 into pPD95.86 (Fire Vector kit 1995). pJH617, pJH636 and pJH841 are deletions of pJH510, expressing NAB-1Δ1-190, NAB-1Δ204-387 and NAB-1Δ286-387, respectively. *Punc-25*-SNB-1::mRFP (pJH505) was constructed by inserting the SNB-1 sequences into *Punc-25* mRFP. pJH439 and pJH470 are N-terminal mRFP-fusion expression plasmids with a *sad-1* mini-gene C4EA (Crump et al., 2001) and the *unc-10* genomic sequence inserted into *Punc-25* mRFP, respectively. pJH101 was generated by inserting the *Punc-115* promoter in front of the *sad-1* mini-gene C4EA. The SAD-1ΔDKV expression vector (pJH447) was created by mutating K910 to a stop codon and subcloned into pJH101. pJH713 and pJH714 were made by inserting cDNA for the SAD-1 long- and short-isoforms behind *Punc-25*, respectively. The bait construct for the yeast

two-hybrid screen was generated by ligating the *sad-1* cDNA fragment into the pGKBT7 plasmid (Clontech, Mountain View, CA). pJH164, pJH179, pJH180, pJH181 and pJH186 express LexA fused to SAD-1 amino acids 565-914, 306-584, 581-730, 730-914 and 306-407, respectively. pJH200 is a prey plasmid containing NAB-1 cDNA encoding the PDZ domain in pACT2 (Clontech, Mountview, CA). The *unc-30* RNAi plasmid pJH573 was generated by inserting a 0.7 kb *unc-30* cDNA fragment into pPD129.36 (Fire Vector kit, 1999).

Yeast two-hybrid screen
A yeast two-hybrid screen was performed as described in the Matchmaker protocol (Clontech, Mountain View, CA). 1.8×10^6 clones were screened on HIS^- plates with 50 mM 3-amino triazole and for the activation of lacZ expression.

Biochemistry and immunofluorescent stainings
Three recombinant proteins consisting of overlapping regions of SAD-1 (amino acids 280-565, 406-585 and 565-914) fused to glutathione S-transferase (GST) were used to immunize a goat to generate the anti-SAD-1 antibody (Covance, Denver, PA) and affinity-purify the antibody. Whole-mount staining, *C. elegans* lysate preparation, western blotting, immunoprecipitation and GST pull-down assays were performed as described previously (Liao et al., 2004).

Transgenic-animal generation
All GFP and mRFP-tagging constructs were co-injected with the LIN-15 expression vector into *lin-15(n765)* animals. Stable transgenic lines were obtained after UV irradiation of animals carrying the desired extra-chromosomal arrays and backcrossed to N2 four times. All rescuing experiments were performed by co-injecting the rescuing plasmid (20 ng/ml) with the *Podr-1*-GFP marker into mutant animals.

RNA interference
Double-stranded RNA (dsRNA) was synthesized from pJH573 as described (Fire et al., 1998) and injected at 40 μg/ml dsRNA. Young adult F1 animals that lost GFP signals in all six DD cell bodies but retained all 13 GFP-positive VD-neuron cell bodies were scored for the dorsal and ventral GFP synapse puncta.

RESULTS
Mutations in *sad-1* cause defects in both neuronal polarity and synapse formation
In *C. elegans sad-1* loss-of-function mutants, a presynaptic vesicle marker, SNB-1::GFP, distributes more diffusely at synapses and accumulates ectopically in the dendritic regions of the DD-type GABAergic motoneurons in the first larval (L1) stage (Crump et al., 2001). This suggests a role for SAD-1 in regulating both synapse morphology and specifying neurite identity in DD neurons. We further examined the role of *sad-1* in neuronal polarity throughout development.

In wild-type L1 animals, only embryonically born DD-type GABAergic neurons are present and synapse onto ventral muscles. At the end of L1, the ventral DD synapses are removed and new DD synapses are established with dorsal muscles (White et al., 1978). VD-type GABAergic neurons, born at the end of the L1 stage, form synapses with the ventral muscles. This rewiring of GABAergic neurons can be observed using a presynaptic vesicle marker, *juIs1*, which expresses SNB-1::GFP under the GABAergic neuron promoter *unc-25* (*Punc-25*) that is active in both DD and VD neurons (Hallam and Jin, 1998). In wild-type L1 animals, *juIs1* puncta are present along the ventral cord only (Fig. 1A, upper panels), representing synapses by DD neurons along the ventral body muscle. From the second larval stage onward, fluorescent puncta are observed on both the ventral and dorsal sides, representing dorsal synapses by DD neurons and ventral synapses by VD neurons.
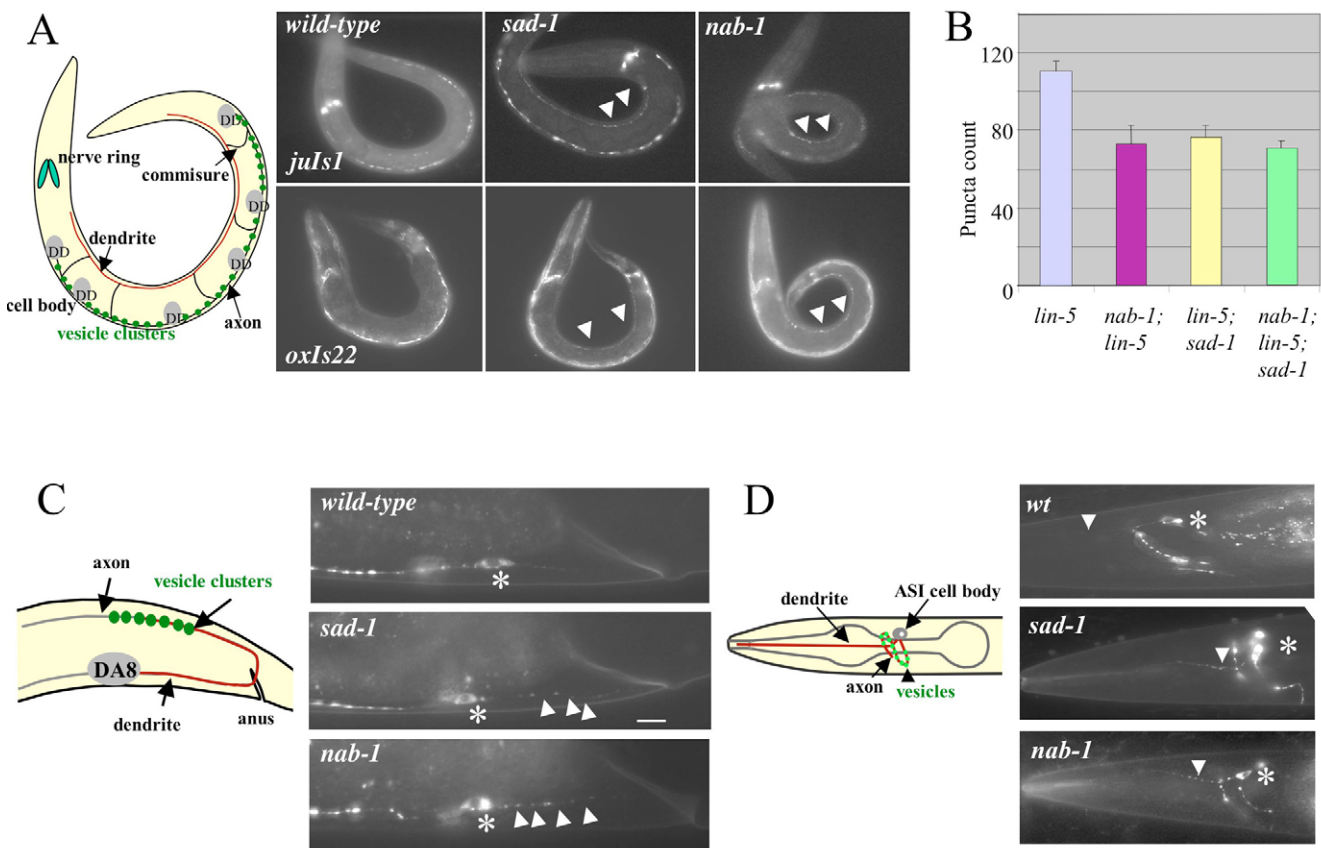
Fig. 1. Loss of *sad-1* and *nab-1* functions lead to polarity defects in various neurons. (**A**) L1-stage *sad-1* and *nab-1* animals have DD polarity defects. Arrowheads indicate the ectopic dorsal SNB-1::GFP (*juIs1*) or UNC-49B::GFP (*oxIs22*) signal. A schematic diagram of the normal connectivity of DD neurons in L1 is shown on the left of the images. (**B**) *sad-1* and *nab-1* mutations lead to a decreased number of DD synapses in adult-stage *C. elegans*. The number of *juIs1* puncta on the dorsal nerve cord of *nab-1;lin-5*, *lin-5;sad-1* and *nab-1;lin-5;sad-1* animals was compared with *lin-5* animals (*n*>15 animals, *P*< 0.001 by Tukey-Kramer multiple comparison test). (**C**) Polarity defects in a DA8 cholinergic motoneuron of *sad-1* and *nab-1* shown by SNB-1::GFP (*wdIs20*). *sad-1* and *nab-1* animals show SNB-1::GFP puncta in the dendritic region of the neuron (arrowheads). *DA8 cell body. (**D**) ASI chemosensory neurons are visualized using the *Pstr-3* SNB-1::GFP vesicle marker (*kyIs105*). Wild-type animals shows discrete vesicle clusters along the axon, but none in the dendritic process (arrowhead). Both *sad-1* and *nab-1* animals show puncta in the dendritic and axonal processes. *ASI-neuron cell body. Scale bar: 5 μm in C.

Consistent with a previous report on *sad-1(ju53)* mutants (Crump et al., 2001), we found that *ky289*, a protein-null allele of *sad-1* (Crump et al., 2001), and two kinase-defective alleles, *hp119* (D187N) and *hp124* (G64E), also displayed both dorsal and ventral *juIs1* puncta at the L1 stage (Fig. 1A, top panels, not shown for *hp119* and *hp124*). We further examined whether this failure in restricting the localization of presynaptic proteins is accompanied by a similar ectopic accumulation of post-synaptic components. Using *oxIs22*, a fluorescent GABA-receptor marker (UNC-49B::GFP), we observed a corresponding ectopic accumulation of postsynaptic-receptor clusters on dorsal muscles in L1 *sad-1* mutants, suggesting that these ectopic dorsal synaptic-vesicle clusters represent functional synapses (Fig. 1A, lower panels). Therefore, DD neurons fail to restrict axonal fate in neurites, forming synapses with both dorsal and ventral muscles in L1 larval-stage *sad-1* mutants.

After the L1 stage, the *juIs1* marker is expressed in both DD and VD GABAergic neurons. To examine exclusively the polarity of DD neurons in later developmental stages, we eliminated VD neurons using a *lin-5* mutation, which specifically abolishes all post-embryonic cell divisions, including the events that give rise to VD neurons (Horvitz et al., 1983; Lorson et al., 2000). Adult *lin-*

5(e1348) animals carrying *juIs1* displayed 110.6±5.2 (*n*=15) fluorescent puncta exclusively along the dorsal cord. In adult *lin-5; sad-1* animals, synapses were observed only on the dorsal cord (data not shown), suggesting the polarity defect of DD neurons observed at the L1 stage was corrected by the remodeling event. However, in these animals, the number of dorsal synapses was reduced to 76.6±6.0 (*n*=15, *P*<0.001; Fig. 1B).

To examine the effect of *sad-1* mutations on the polarity of VD neurons that synapse with ventral muscles, we eliminated the expression of *juIs1* in DD neurons using a RNA interference (RNAi) method (Hallam et al., 2002). UNC-30 is a GABAergic neuron-specific transcription factor (Eastman et al., 1999) that activates the *Punc-25* used for driving *juIs1* expression. Injection of double-stranded RNA (dsRNA) against *unc-30* at specific concentrations selectively eliminates transcription from the *Punc-25* promoter in DD neurons and therefore allows for visualization of SNB-1::GFP in VD synapses alone.

In wild-type animals carrying the *juIs1* marker, injection of *unc-30* dsRNA eliminated GFP signals from DD cell bodies and all synaptic puncta on the dorsal cord (Fig. 2A, wt panels) without affecting the GFP signal in VD cell bodies (Fig. 2B, wt panels). In *sad-1* mutants, injection of *unc-30* dsRNA at the same
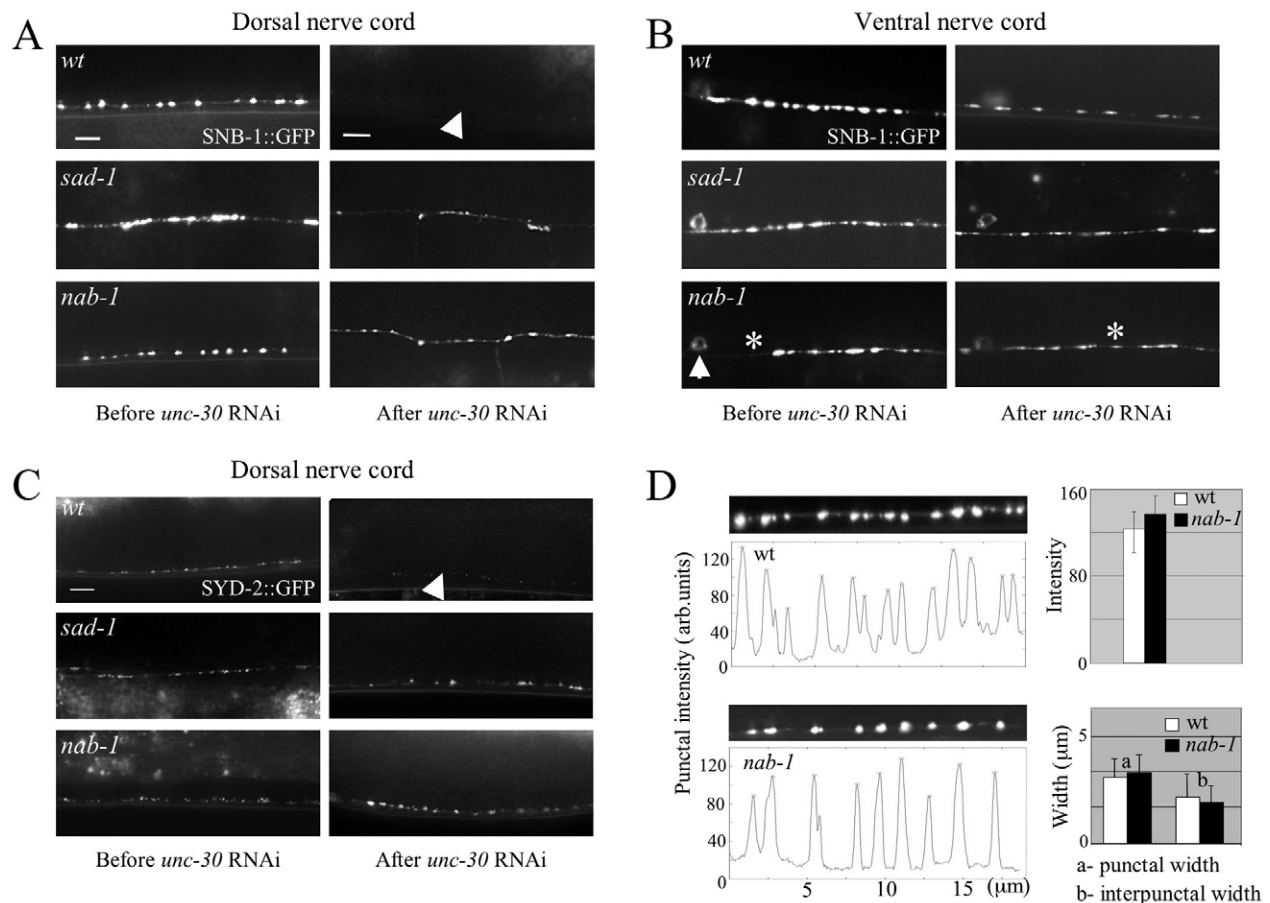
Fig. 2. *sad-1* and *nab-1* mutants fail to restrict axonal fate in VD neurons. (**A**) GABAergic synapses along the dorsal cord in wild-type, *sad-1*- and *nab-1*-mutant young adults visualized by *juIs1* marker. *nab-1* mutants show no synaptic morphology defects. After *unc-30* RNAi treatment to block *juIs1* expression in DD neurons, ectopic synaptic-vesicle clusters in VD neurons were detected in both *nab-1* and *sad-1* mutants. Arrowhead shows the dorsal nerve cord. (**B**) *nab-1* mutants have a reduced number of synapses along the axon of VD neurons before and after *unc-30* RNAi treatment. Arrow shows VD neuron cell body. (**C**) *nab-1* and *sad-1* mutants display ectopic dorsal SYD-2::GFP, an active-zone marker, in VD neurons. Arrowhead shows the dorsal nerve cord. (**D**) *juIs1* phenotypes in wild-type (wt, left upper panels) or *nab-1* (left lower panels) animals were analyzed with MathLab software (developed by C. Mok, University of Toronto, Canada). The intensity and width of individual fluorescent punctum, as well as the distance between puncta (inter-punctal width), was calculated from *juIs1* images of wild-type and *nab-1* animals. Left panels; a graphical representation and the corresponding *juIs1* image. Average values of the punctal intensity (upper right panel), punctal width (lower right panel) and interpunctal width (lower right panel) were plotted and shown. No significant difference was found between wild-type and *nab-1* values (*n*=13, *P*>0.05). Scale bar: 5 μm in A,C.

concentration also eliminated the GFP signal in DD cell bodies. However, 72.5±8.7 (*n*=15) puncta remained along the dorsal side, suggesting that VD neurons fail to restrict synaptic-vesicle transport to their dendrites (Fig. 2A, *sad-1* panels). Similarly, these VD neurons also displayed an ectopic distribution of two active-zone protein markers, UNC-10::GFP and SYD-2::GFP, expressed in GABAergic neurons. After *unc-30* RNAi injection, UNC-10::GFP and SYD-2::GFP signals were diminished completely from the DD-neuron cell bodies in both wild-type and *sad-1*-mutant animals. However, intense dorsal SYD-2::GFP (Fig. 2C, wt and *sad-1* panels) and UNC-10::GFP (data not shown) puncta remained specifically in *sad-1* mutants. Therefore, VD neurons fail to restrict axonal fate in neurites in *sad-1* mutants. In addition, a mild but statistically significant decrease of normal ventral synapses was observed in VD neurons in *sad-1* mutants (130.3±8.4 for *hp124* and 123.8±10.2 for *ky289* versus 143.7±13.1 for wild-type, *n*=15, *P*<0.01; Fig. 2B, *sad-1* panels). Together, these data indicate that *sad-1* mutations cause polarity defects in both DD and VD neurons.

Mutations in *sad-1* cause polarity defects in cholinergic motoneurons and chemosensory neurons

We examined whether the polarity defects of *sad-1* loss-of-function mutants is restricted to GABAergic motoneurons. The *wdIs20* marker expresses SNB-1::GFP in the VA and DA classes of cholinergic motoneurons from the *unc-4* promoter (Miller, III and Niemeyer, 1995). The ventrally located DA8 motoneuron extends a neurite posteriorly, which turns dorsally to join the dorsal nerve cord, where it adopts the axonal fate and forms synapses with dorsal muscles and VD motoneurons. The posteriorly extended ventral process is postsynaptic to several interneurons (White et al., 1986). In a wild-type genetic background, a majority of the animals (87.9%, *n*=74) showed no ventral SNB-1::GFP puncta posterior to the DA8 cell body along the ventral dendritic process. By contrast, only 32.1% of *sad-1*-mutant animals displayed wild-type DA8 morphology, whereas the rest showed 3-4 puncta posterior to the DA8 cell body (*n*=131; Fig. 1C), indicating an ectopic accumulation of synaptic vesicles to the dendritic region of DA motoneurons.

We also examined neuronal polarity in ASI chemosensory neurons that display morphologically distinct dendrites and axons. The short axon from each ASI neuron forms 7-13 en passant synapses with interneurons in the nerve ring while a single long dendritic process extends from the cell body to the tip of the nose where it ends in a ciliated opening (White et al., 1986). This wiring pattern can be directly visualized by the *Pstr-3*-SNB-1::GFP (*kyIs105*) marker (Fig. 1D) (Crump et al., 2001). We found that 52% of *sad-1* mutants (*n*=70) displayed dim and diffuse fluorescent puncta along the dendrite, whereas only 11% (*n*=80) of wild-type animals displayed a sporadic dendritic GFP signal (Fig. 1D). Taken together, we conclude that, in addition to the previously reported severe diffusion of synaptic vesicles, loss of SAD-1 function also leads to the disruption of neuronal polarity in multiple neuron types.

NAB-1 physically interacts with SAD-1 in vitro and in vivo

To investigate the mechanisms through which *sad-1* regulates neuronal polarity and synapse morphology, we performed a yeast two-hybrid screen to identify SAD-1-interacting proteins. Although both the kinase domain of SAD-1 and its C-terminal non-catalytic regions are essential for SAD-1 function (Crump et al., 2001), we chose the non-catalytic region (amino acids 283-914) of the predicted SAD-1 protein as the bait for the screen. We isolated 34 clones representing eight genes that code for proteins interacting with different regions of the non-catalytic domain of SAD-1.

One of these genes encodes NAB-1, the sole *C. elegans* homolog of the Neurabin and Spinophilin scaffolding-protein family. By deletion analysis, we determined that the C-terminal region of SAD-1 (amino acids 730-914) mediates this interaction with NAB-1 (Fig. 3A). Because the SAD-1 C-terminus contains a consensus PDZ-binding sequence (Asp-Lys-Val-COOH or DKV motif), and NAB-1 contains a PDZ domain, we tested the ability of this PDZ domain to bind directly to SAD-1 baits. The PDZ domain alone was sufficient to bind full-length SAD-1 (data not shown). Furthermore, deletion of the DKV motif of SAD-1 completely abolished the bait-prey interaction of SAD-1 to either NAB-1 (Fig. 3A) or NAB-1 PDZ domain (data not shown), suggesting that this motif mediates the interaction between SAD-1 and NAB-1 in vitro.

The interaction between NAB-1 and SAD-1 was further confirmed by GST pull-down assays. GST alone and GST fused with either full-length NAB-1 (GST-NAB-1) or with the NAB-1 PDZ domain (GST-PDZ) were used to precipitate interacting proteins from *C. elegans* total-protein extracts (Fig. 3B). In *C. elegans* lysates, anti-SAD-1 antibody recognizes two protein bands, 100 and 110 kD. These two forms were also observed using an anti-FLAG antibody when a FLAG-tagged SAD-1 mini-gene was expressed from the pan-neuronal promoter *Punc-115* (Fig. 3B). Both full-length NAB-1 and the PDZ domain of NAB-1 specifically precipitated the 110 kD form of SAD-1 or FLAG-tagged SAD-1 (Fig. 3B). The 100 kD band represents a previously unknown isoform of SAD-1 that lacks the last 89 amino acids, including the consensus PDZ-binding site (Fig. 3D).

To determine whether SAD-1 and NAB-1 interact in vivo, we generated a stable transgenic strain, *hpIs66*, which carries a fully functional GFP-tagged *nab-1* genomic clone (data not shown). Immunoprecipitating NAB-1::GFP from total-protein lysates of *hpIs66* using an anti-GFP antibody also brought down the 110 kD SAD-1 isoform specifically (Fig. 3C, center panels). Conversely, immunoprecipitation using an anti-SAD-1 antibody precipitated

NAB-1::GFP from *hpIs66* lysate, but not from *sad-1(ky289);hpIs66* lysate (Fig. 3C, right panels). Our data show that SAD-1 and NAB-1 physically interact in vivo as well as in vitro.

nab-1 encodes multiple isoforms that are expressed in epithelia and in the nervous system

In the *hpIs66* strain that carries functional NAB-1::GFP, GFP was inserted in-frame in the C-terminus, shared by all predicted NAB-1 isoforms with the exception of C43E11.6c (Fig. 4). In western blot analysis using antibodies against GFP, we consistently detected three major forms of NAB-1::GFP that corresponded to the predicted molecular weight of the two longest isoforms, and one band that migrated slower than any of the predicted isoforms (Fig. 3C, left lanes). A deletion allele, *ok943*, deletes exons 7 to 9 of the *nab-1* gene, resulting in a premature stop codon immediately following the PDZ domain in all detectable isoforms (Fig. 4). This allele was used for all our subsequent biochemical, genetic and functional analyses.

We used *hpIs66* to determine NAB-1 expression during development. NAB-1::GFP expression is restricted to epithelia and neurons. The earliest expression was observed in the hypodermis of 2-fold-stage early embryos (Fig. 5A,B). Immediately prior to hatching, this expression became restricted to the epithelial excretory canal (Fig. 5C-E) and the nervous system, including the central nervous system (nerve ring, Fig. 5C) and the motoneurons (dorsal and ventral nerve cords, Fig. 5D-G). In L3 and L4 larvae, NAB-1::GFP also localized transiently at the membranes of the developing vulva epithelia (Fig. 5E).

NAB-1 co-localizes with SAD-1 at the presynaptic terminals in mature neurons

SAD-1 is expressed exclusively in the nervous system, and therefore shares an overlapping expression pattern with NAB-1 in neurons. In *hpIs66* animals, NAB-1::GFP appears punctate along the dorsal and ventral nerve cords (Fig. 5F,G and Fig. 6A), indicative of enrichment at synaptic regions. We examined the subcellular localization of NAB-1::GFP by co-immunostaining with antibodies against various presynaptic proteins.

We found that NAB-1::GFP puncta partially co-localized with the synaptic-vesicle protein SNT-1 (Fig. 6A, left panels) and the active-zone protein UNC-10 (Fig. 6A, right panels), suggesting that NAB-1 is present in presynaptic regions that are associated with vesicle pools and active zones. Similar to NAB-1, SAD-1 also showed co-localization with SNT-1 (Fig. 6B, left panels), and a close association with UNC-10 (Fig. 6B, right panels). NAB-1::GFP and SAD-1 also showed partial co-localization, where each NAB-1::GFP punctum was associated with SAD-1 staining (Fig. 6C).

In the *C. elegans* nervous system, synapses formed by adjacent axons in nerve bundles overlap with each other, preventing examination at single-synapse resolution. To examine SAD-1 and NAB-1 localization patterns at the single-synapse level, we co-expressed the GFP-tagged largest isoform of NAB-1 and mRFP-labeled synaptic proteins in GABAergic neurons using the *Punc-25* promoter (Eastman et al., 1999; Liao et al., 2004; Yeh et al., 2005). Consistent with the whole-mount staining pattern, *Punc-25*-NAB-1::GFP showed partial co-localization with *Punc-25*-UNC-10::mRFP (Fig. 6D, left panels) and *Punc-25*-SNB-1::mRFP (Fig. 6D, right panels). *Punc-25*-SAD-1::mRFP showed complete co-localization with *Punc-25*-SNB-1::GFP (Fig. 6E, left panels), and partial co-localization with *Punc-25*-UNC-10::GFP (Fig. 6E, right panels). We observed a complete co-localization of *Punc-25*-NAB-1::GFP and *Punc-25*-SAD-1::mRFP fluorescent puncta (Fig. 6F), further supporting the idea of a direct interaction between these two

proteins. The increased colocalization of NAB-1::GFP and SAD-1::RFP in GABAergic neurons compared with in whole-mount staining may be partially due to the overexpression of two interacting proteins.

nab-1 regulates polarity in *C. elegans* neurons

If interactions between NAB-1 and SAD-1 are required for their biological functions, mutations in these two genes might result in similar phenotypic defects. Unlike *sad-1* mutants, in which synaptic-vesicle clusters are diffuse, we observed fairly normal-shaped synaptic-vesicle clusters in GABAergic (Fig. 2A, *nab-1* panels) neurons. Quantitative comparison of the intensity, shape and density

of fluorescent vesicle puncta did not show any significant differences between wild-type and *nab-1* animals (Fig. 2D). We did not observe any change in synapse morphology in cholinergic and ASI chemosensory neurons in *nab-1* mutants either (data not shown), suggesting that *nab-1* is not required for synapse morphology in these neurons.

In contrast to the normal synapse morphology, we observed severe polarity defects in *nab-1* mutants. DD motoneurons in L1-stage *nab-1* mutants formed ectopic synapses on dorsal muscles (100%, $n=100$; Fig. 1A, right panels). As in *sad-1* mutants, the DD-polarity defect in *nab-1* mutants was also corrected after L1 rewiring, but fewer synapses were made (73.1±9.7, $n=18$, $P<0.001$)
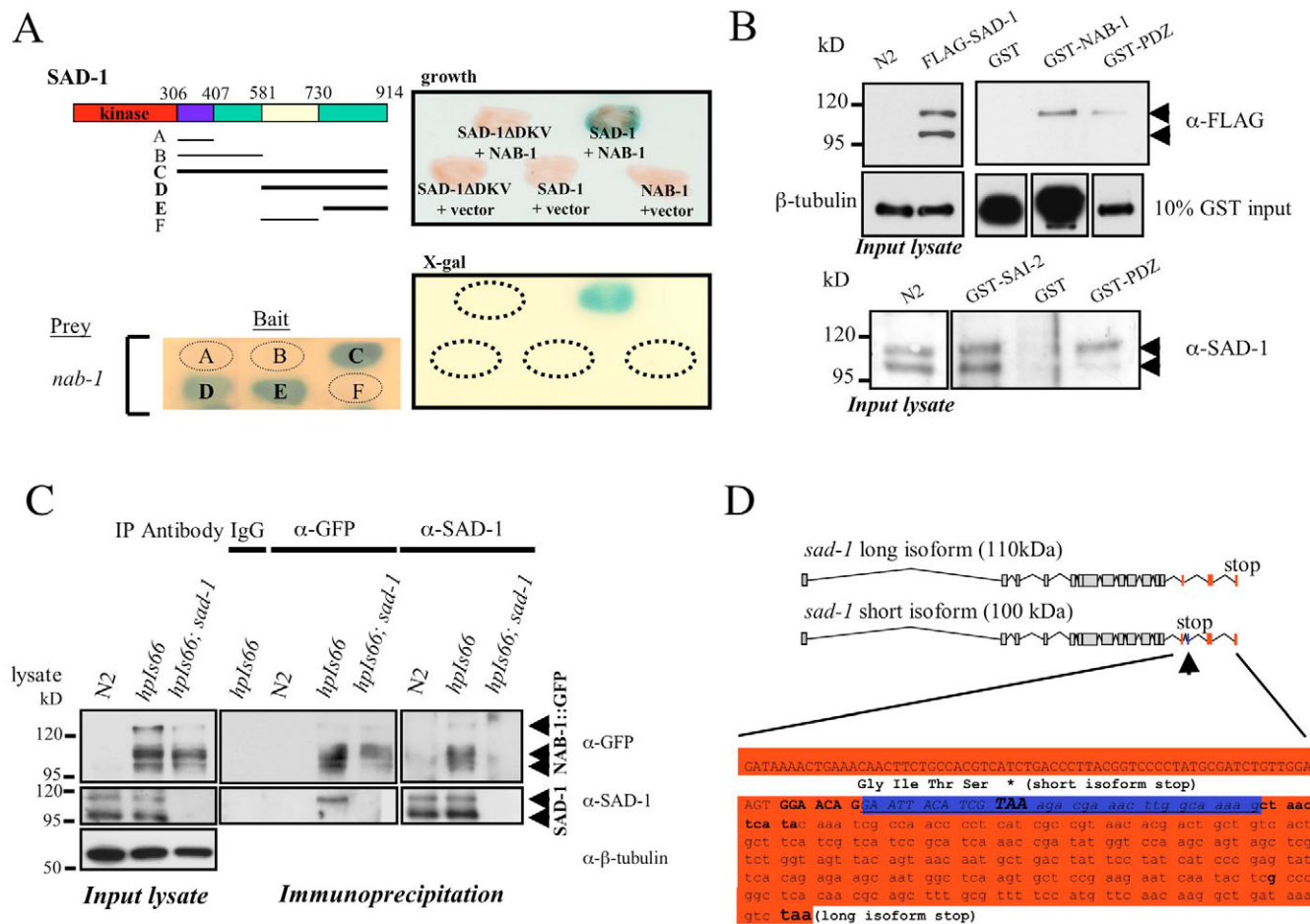

Fig. 3. SAD-1 and NAB-1 interact in vitro and in vivo. (**A**) Yeast two-hybrid assays to determine the NAB-1-interacting domain of SAD-1. Upper left panel; schematic representation of SAD-1 deletions used to map the region for NAB-1 interaction. Lower left panel; Y274 yeast strain was co-transformed with a NAB-1-AD prey plasmid and various LexA-SAD-1-deletion bait plasmids, and tested for β-gal activity on X-gal plates. Blue color indicates interaction. Right panels; yeast transformed with different bait- and prey-plasmid combinations (as indicated) were grown in trp− leu− SD media, and color development with X-gal allowed to occur. LexA-SAD-1 amino acids 280-914 (SAD-1) or LexA-SAD-1 amino acids 280-911 (SAD-1ΔDKV) were used as bait and NAB-1 as prey. The lacZ reporter was expressed in only yeast strains carrying both full-length SAD-1 and NAB-1. (**B**) GST-pull-down assays showed that GST-NAB-1 (or the PDZ domain) selectively interacts with the 110 kD isoform of SAD-1. Upper panels; GST, GST-NAB-1 PDZ domain and GST-full-length NAB-1 precipitated FLAG-tagged SAD-1 from the total-protein lysate from *C. elegans* strains carrying an integrated, fully functional SAD-1::FLAG array. Lysate input and GST input are shown at the bottom. Lower panel; GST, GST-SAI-2 and GST-NAB-1 PDZ precipitated endogenous SAD-1 from wild-type *C. elegans* lysate. SAI-2, another SAD-1-interacting protein identified from the yeast two-hybrid screen, pulled-down both isoforms of SAD-1, whereas NAB-1 precipitated only the 110 kD isoform. (**C**) Co-immunoprecipitation experiments showed that SAD-1 and NAB-1 interact in vivo. *C. elegans* lysates prepared from wild type, *hpIs66* or *hpIs66*; *sad-1* were immunoprecipitated with either anti-SAD-1 or anti-GFP antibody (for NAB-1::GFP), probed with anti-GFP antibody and then stripped and re-probed with anti-SAD-1 antibody, or vice versa. (**D**) Two alternatively spliced forms of *sad-1*. Schematic representation of the two splice variants encoded by the *sad-1* gene is shown. We sequenced all the existing cDNA clones of *sad-1* and discovered that two clones (yk134f11 and yk238h3) in which an additional exon was present in the C-terminal region of the clone, which leads to an earlier stop than the predicted SAD-1 coding region. The corresponding amino acid sequence truncated in this short isoform is shown.
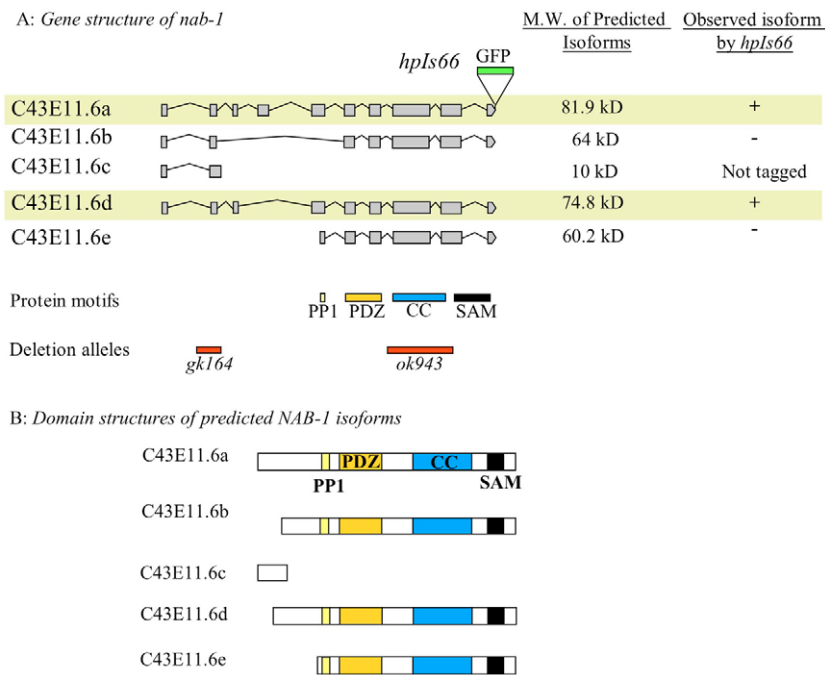
A: *Gene structure of nab-1*

Fig. 4. Gene structure of *nab-1* and the domain structures of its predicted isoforms. (**A**) Predicted multiple isoforms encoded by the *nab-1* gene. The expected molecular weight of each isoform is listed. Grey boxes; exons. Lines; introns. *hpIs66* transgenic animals carry an integrated array of a construct where GFP sequence was inserted at the 3' end of the *nab-1* gene just before the stop codon. The genetic lesion of the two *nab-1*-deletion mutants, *gk164* and *ok943*, are shown. (**B**) The predicted isoforms of NAB-1 contain multiple protein motifs, except isoform c. The domain structures of the predicted isoforms of NAB-1 are shown schematically. The shortest isoform, C43E11.6c, does not contain any known protein motif.

compared with wild-type animals (110.6±5.2; Fig. 1C). In VD motoneurons, we also observed an ectopic accumulation of presynaptic-vesicle clusters (50.0±6.2, *n*=15; Fig. 2A, *nab-1* panels), as well as an ectopic accumulation of the active-zone proteins SYD-2::GFP (Fig. 2C, *nab-1* panels) and UNC-10::GFP (not shown) along the dorsal cords of *nab-1* mutants. A decrease in the number of normal synapses along the ventral axonal process was also observed in *nab-1* mutants (96.6±11.5, *n*=15, *P*<0.001; Fig. 2B, *nab-1* panels).

The polarity of other classes of neurons is also affected in *nab-1* mutants. Similar to *sad-1* mutations, we observed an accumulation of 3-4 ectopic presynaptic-vesicle clusters in the dendritic process of the DA8 cholinergic motoneuron in *nab-1* mutants using the *wdIs20* marker (98.2%, *n*=58; Fig. 1C, *nab-1* panel). In ASI

chemosensory neurons, 86% of *nab-1* animals (*n*=80) accumulated bright presynaptic-vesicle clusters in the dendrites when examined by *kyIs105* (Fig. 1D). As opposed to *sad-1* mutants, in which the ectopic synaptic-vesicle clusters are dim and diffuse, all the ectopic vesicle clusters were discrete and normal in morphology in *nab-1* mutants (Fig. 1D), supporting a specific role of *nab-1* in neuronal polarity.

To determine whether NAB-1 functions cell-autonomously in regulating neuron polarity, we tested whether the polarity defects in VD neurons can be rescued by the specific expression of NAB-1 in GABAergic neurons. Expression of the largest isoforms of NAB-1 from *Punc-25* in *nab-1*-mutant animals eliminated ectopic VD dorsal-synapse formation to the same degree as rescues by a full-length *nab-1* genomic construct or by expression of the largest isoforms of NAB-1
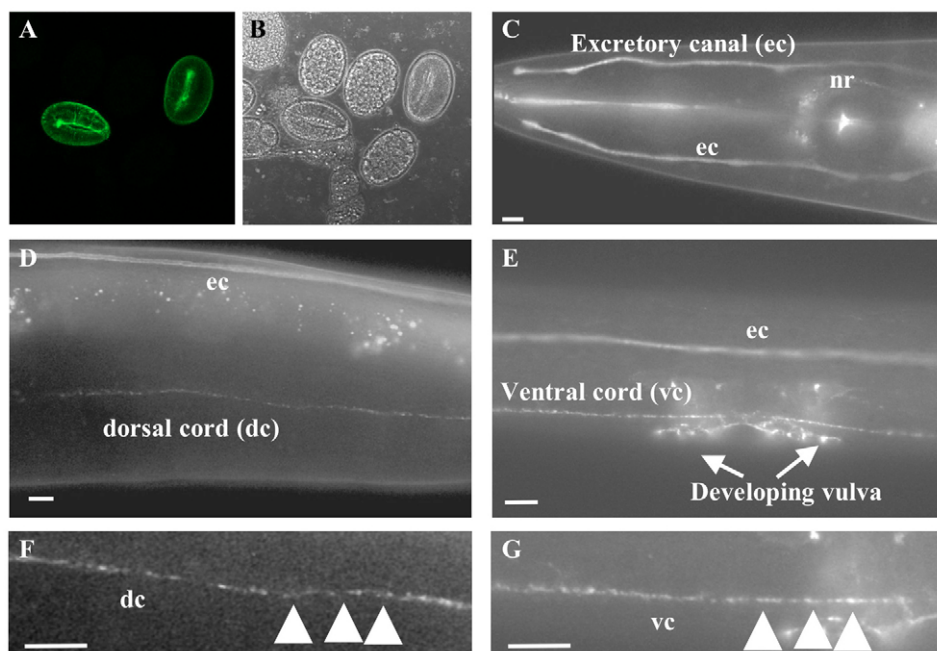

Fig. 5. NAB-1::GFP is expressed in epithelia and in the nervous system. (**A**,**B**) Embryos carrying NAB-1::GFP from its own promoter (*hpIs66*) are shown with fluorescence (A) or DIC (B) microscopy. (**C-E**) *hpIs66* animals express NAB-1::GFP in the nervous system (nerve ring, and dorsal and ventral nerve cord) and excretory canal. By the L4 stage, NAB-1::GFP is also seen in the developing vulva (E). (**F**,**G**) Enlarged portions of the dorsal nerve cord from D, and ventral cord from E are shown. Arrowheads show punctate expression pattern of NAB-1::GFP. Scale bar: 5 μm. ec, excretory canal; nr, nerve ring; vc, ventral cord; dc, dorsal cord.
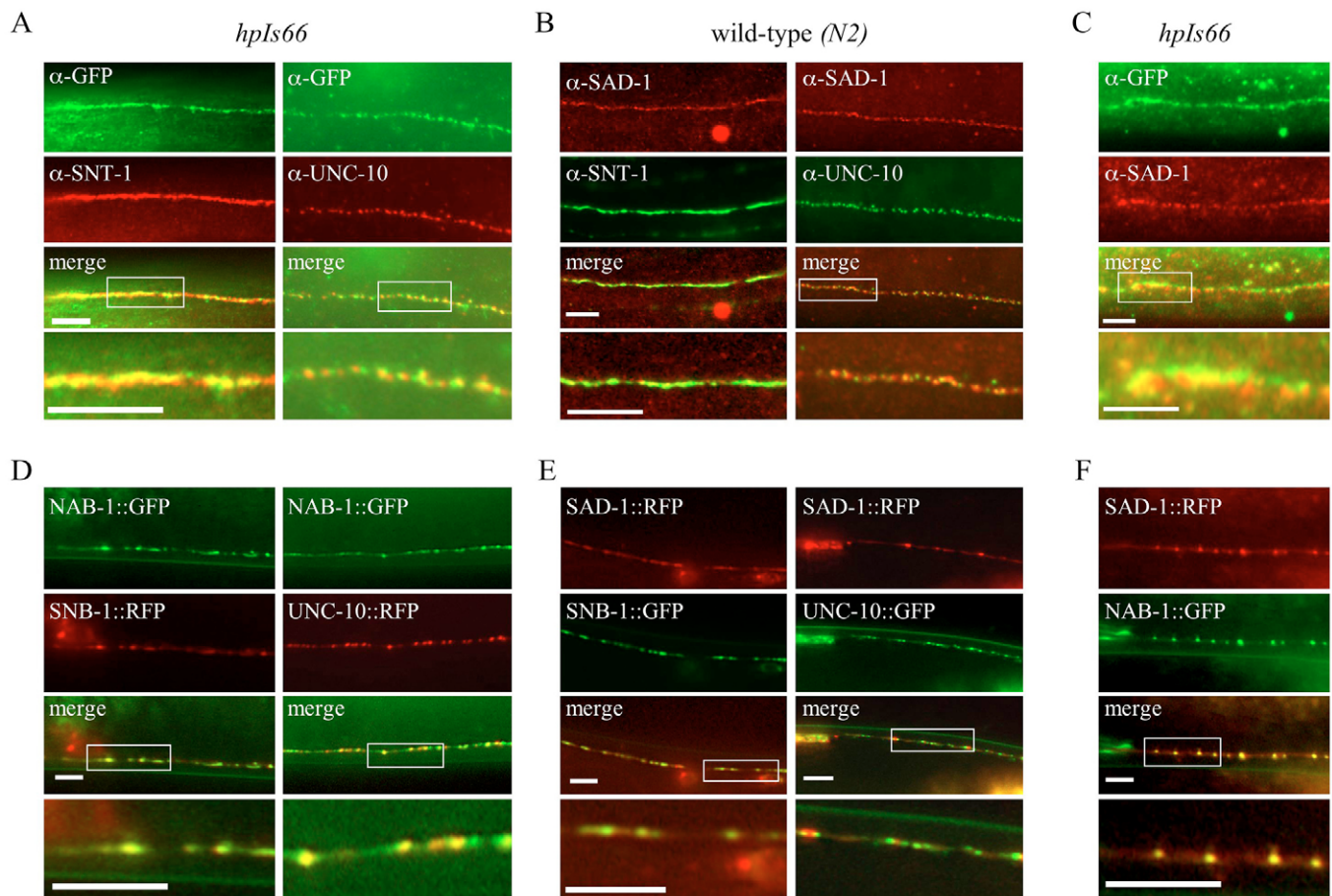
Fig. 6. NAB-1 is a presynaptic protein and partially co-localizes with SAD-1. (**A**) *hpIs66* animals were co-stained with anti-GFP antibody (green) and either anti-SNT-1 (red, left panels) or anti-UNC-10 (red, right panels). (**B**) Wild-type animals co-stained with anti-SAD-1 antibody (red) and either anti-SNT-1 (green, left panels) or anti-UNC-10 (green, right panels). (**C**) *hpIs66* animals were co-stained with anti-GFP (green) and anti-SAD-1 antibodies (red). (**D**) Young adult animals co-expressing SNB-1::mRFP (red) and NAB-1::GFP (green, left panels) or UNC-10::mRFP (red) and NAB-1::GFP (green, right panels) in GABAergic neurons. (**E**) Young adult animals co-expressing SAD-1::mRFP (red) and SNB-1::GFP (green) (left panels) or SAD-1::mRFP (red) and UNC-10::GFP (green) (right panels) in GABAergic neurons. (**F**) Wild-type animals co-expressing SAD-1::mRFP (red) and NAB-1::GFP (green) in GABAergic neurons. Last panels of each column show the enlarged image of areas indicated by white boxes. Scale bar: 5 μm.

from the pan-neuronal promoter (*Punc-115*) (Fig. 7). The same NAB-1 isoform expressed by the muscle-specific promoter *Pmyo-3* failed to rescue any defects (Fig. 7). Similarly, we observed the same rescues of ventral synapse numbers when NAB-1 was expressed in neurons using different neuron-specific promoters, but not the muscle-specific promoter. Wild-type animals have 141.75±13.1 (*n*=15) ventral synapses, whereas *nab-1* mutants displayed 95.5±11.2 (*n*=17) ventral synapses (*P*<0.001). Expression of NAB-1 from neuron-specific promoters or from the genomic *nab-1* construct (*Punc-25*, 125.6±6.9, *n*=15; *Punc-115*, 125.3±9.7, *n*=15; *Pnab-1*, 125.6±3.3, *n*=15) in *nab-1* animals can restore the ventral synapse numbers to close to wild-type levels (*P*>0.05). By contrast, NAB-1 expression from the muscle-specific promoter (*Pmyo-3*, 91.8±7.4, *n*=15) displayed a similar number of ventral synapses as *nab-1* mutants (*P*>0.05). Therefore, NAB-1 is required in neurons to regulate their polarity.

Interaction between NAB-1 and SAD-1 is specifically required for neuronal polarity, but dispensable for synaptogenesis

To examine whether the physical interaction between NAB-1 and SAD-1 is required for establishing neuronal polarity, we generated an in-frame deletion of the PP1-binding site and PDZ domain

(NAB-1Δ204-378), and an in-frame deletion of the PDZ domain alone (NAB-1Δ286-378) in the largest isoform of the *nab-1* gene. Expression of both truncated forms of NAB-1 in GABAergic neurons by *Punc-25* failed to rescue polarity defects or synapse number in VD neurons (Fig. 7). This is in contrast to an in-frame deletion of the non-evolutionarily conserved N-terminal portion of NAB-1 protein (NAB-1Δ1-194), which rescued all defects in VD neurons as effectively as the full-length NAB-1 (Fig. 7). Moreover, we did not find any polarity defects in *gk164*, a *nab-1* deletion mutant that deletes exon 2 of *nab-1* gene (Fig. 4), leading to an in-frame deletion of 30 amino acids in the non-conserved N-terminal region (data not shown). Because *Punc-25*-NAB-1Δ204-378::GFP displayed a similar fluorescent intensity and subcellular localization as the *Punc-25*-full-length NAB-1::GFP (data not shown), we can conclude that the PDZ domain of NAB-1 is specifically required for establishing neuronal polarity.

Mutations in *sad-1* lead to polarity defects, as well as other abnormalities in synapse morphology and axon termination not observed in *nab-1* mutants (Fig. 1D and Fig. 2A,D), suggesting that the interaction between NAB-1 and SAD-1 is specifically involved in establishing polarity. To test this hypothesis, we removed the putative NAB-1-binding motif (DKV) by the insertion
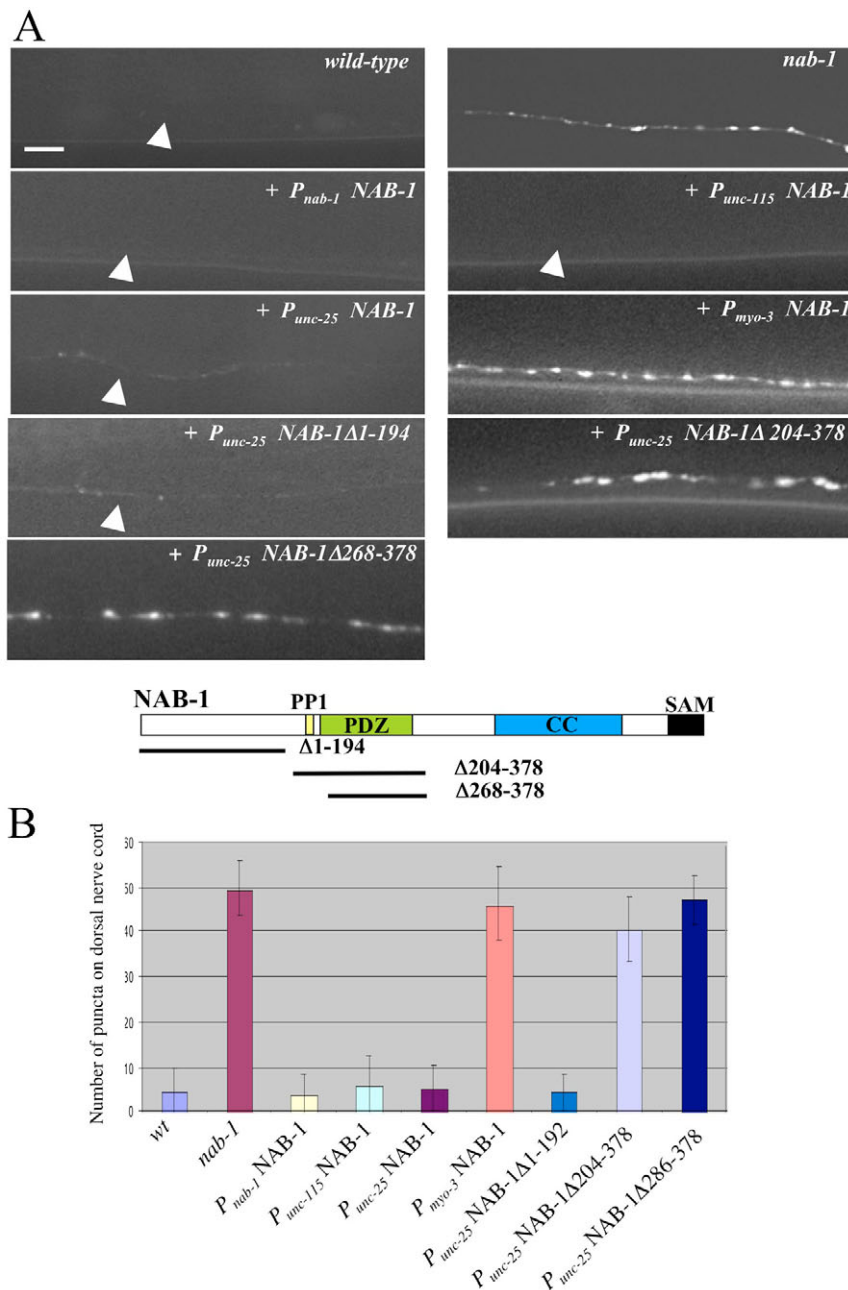
Fig. 7. Neuronal expression of NAB-1 is sufficient to rescue *nab-1* polarity defects.
(**A**) Wild type, *nab-1* mutants and *nab-1* mutants expressing NAB-1 from various promoters, and *nab-1* mutants expressing the NAB-1-deletion constructs were subjected to *unc-30* RNAi treatment. Images of the dorsal SNB-1::GFP vesicle clusters are shown. Diagram (bottom of A) shows NAB-1 deletions used.
(**B**) Quantification of the number of ectopic dorsal SNB-1::GFP puncta per animal (*n*=15). *P*<0.001 (*nab-1*, *Pmyo-3* NAB-1 and *Punc-25* NAB-1Δ204-378 versus wild-type). Scale bar: 5 μm in A.

of a stop codon immediately before the NAB-1-binding site in a SAD-1 mini-gene (SAD-1ΔDKV) and compared its rescuing activity with the original SAD-1 mini-gene. Driven by the pan-neuronal promoter *Punc-115*, the full-length SAD-1 mini-gene fully rescued synaptic morphology of DD synapses (Fig. 8A) and significantly reduced the number of ectopic dorsal synaptic puncta by VDs in *sad-1(ky289)*-null mutants (Fig. 8B and Fig. 7C). By contrast, *Punc-115*-SAD-1ΔDKV failed to reduce the number of ectopic VD synapses (Fig. 8B,C) while fully restoring the morphology of DD (Fig. 8A) and VD (Fig. 8B) synapses, demonstrating that the DKV-mediated SAD-1 interaction with NAB-1 is specifically required for regulating neuronal polarity. The expression of the long isoform of SAD-1 in the GABAergic neurons of *sad-1*-null mutants consistently rescued polarity defects, whereas the expression of the short-form failed to reduce the ectopic dorsal synaptic puncta in VD neurons (Fig. 8E,F).

Therefore, at least in DD and VD GABAergic neurons, we were able to delimit the domain in SAD-1 specifically required for polarity to the PDZ-binding site.

nab-1 and *sad-1* function in the same genetic pathway to control neuronal polarity
The physical interaction and subcellular co-localization of NAB-1 and SAD-1 to synapses, as well as the overlapping polarity phenotypes of *sad-1* and *nab-1* mutants, suggest that these proteins function together to control neuronal polarity. To further test this hypothesis, we examined the genetic interactions between *sad-1* and *nab-1* mutants.

We first quantified and compared the number of ectopic dorsal *juIs1* puncta in VD neurons in *sad-1*, *nab-1* and *sad-1; nab-1* animals after parallel *unc-30* RNAi-treatment. In *sad-1* and *nab-1* mutants, on average, 72.5±8.7 (*n*=15) and 49.7±6.2 (*n*=15) ectopic dorsal-vesicle

DEVELOPMENT

puncta were present per animal, respectively. In *nab-1; sad-1* mutants, only 52.5±6.5 (*n*=15) ectopic puncta were present per animal, which did not reflect an additive or enhancing effect of the two mutations. This lack of enhancement of ectopic dorsal VD synapses is not caused by a 'saturation' level of ectopic synapses; mutation in another neuronal polarity regulator gene, *syd-1*, can further enhance the number of ectopic *juIs1* puncta. In *syd-1* mutants, after *unc-30* RNAi treatment, we observed 56.5±6.0 (*n*=15) ectopic puncta whereas, in *nab-1; syd-1* and *syd-1; sad-1* animals, we observed 87.3±4.5 (*n*=15) and 86.1±5.4 (*n*=15) ectopic puncta, respectively. *syd-1* mutation can even alter the morphology of synaptic-vesicle clusters in *nab-1* and *sad-1* mutants. Synapse morphology of either *nab-1; syd-1* or *syd-1; sad-1* mutants appeared extremely diffuse, unlike any of the single mutants (data not shown). These results are consistent with *nab-1* and *sad-1* functioning in the same genetic pathway.

We observed similar genetic interactions when quantifying defects in DD neurons. After the L1 stage, although the polarity defect of DD neurons had been corrected, the number of DD

synapses in both *sad-1* (73.2±9.7) and *nab-1* (76.6±6.1) mutants was reduced when compared with wild-type animals (110.6±5.2) (Fig. 1B). *nab-1; sad-1* double mutants showed a similar number of synapses in DD neurons (70.7±4.0, *n*=15, *P*<0.001) as either *nab-1*- or *sad-1*-mutant alone (Fig. 1B), further supporting the proposal that *nab-1* and *sad-1* function in the same genetic pathway to regulate neuron polarity.

DISCUSSION

SAD-family kinases contribute to diverse cellular processes, probably through participating in multiple signaling complexes and regulating the phosphorylation of multiple targets. *C. elegans sad-1* mutants display a variety of defects in neuronal development. Here, we reveal that *sad-1* regulates axonal fate and synapse morphology through distinct mechanisms. We provide the first biochemical and genetic evidence that *C. elegans* neurabin (*nab-1*) physically interacts and functions together with *sad-1* to regulate axon-dendrite identity. Furthermore, the NAB-1-SAD-1 interaction is specifically
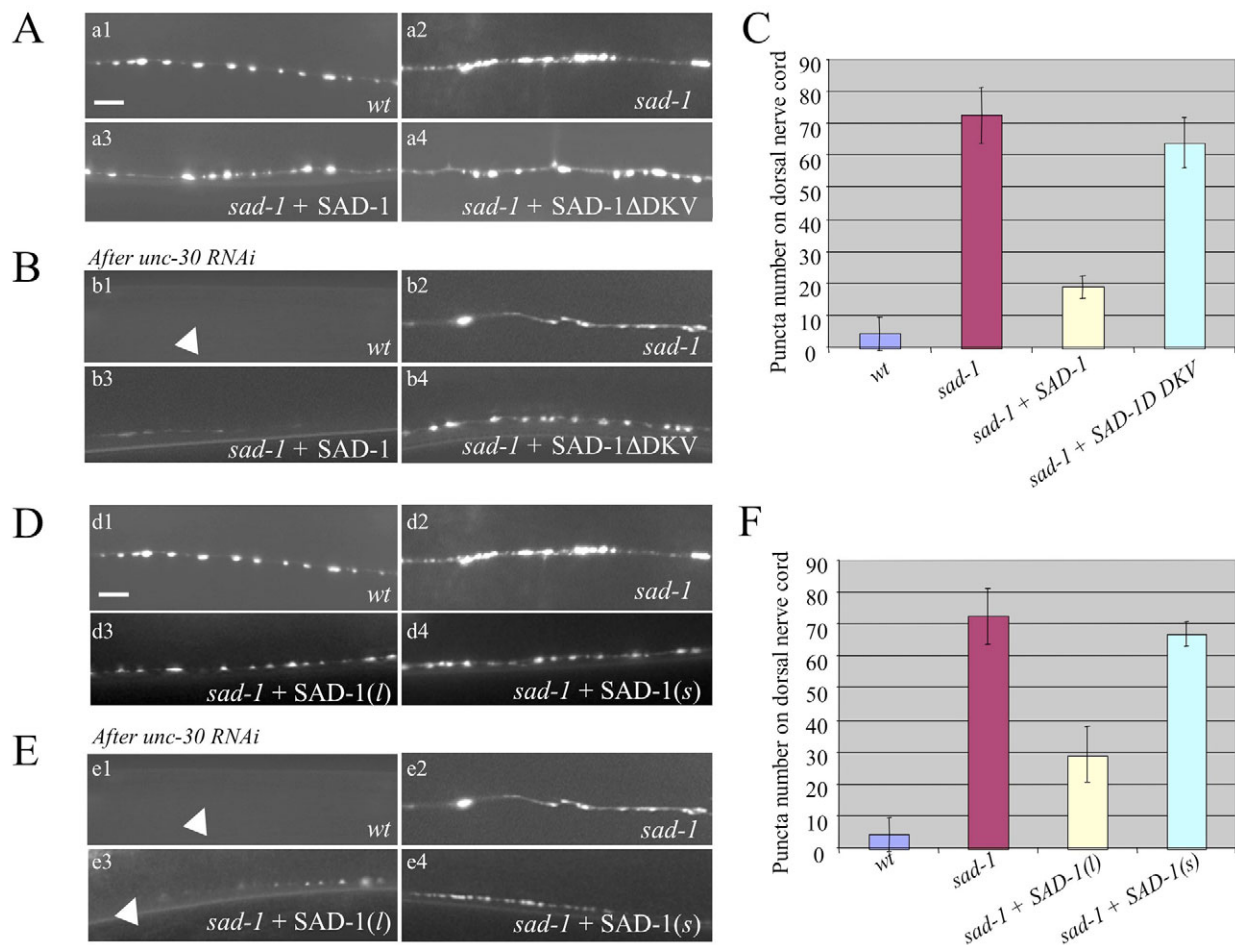

Fig. 8. SAD-1 PDZ-binding site is required for neuronal polarity but not for synaptogenesis. (**A**) SAD-1 lacking the PDZ-binding site rescues synaptic morphology defects. *juIs1* puncta along the dorsal nerve cord of wild-type animals, *sad-1* mutants and *sad-1* animals expressing either SAD-1 (*sad-1+SAD-1*) or SAD-1 lacking PDZ binding site (*sad-1+SAD-1ΔDKV*) from pan-neuronal *Punc-115* are shown. (**B**) SAD-1ΔDKV site fails to rescue *sad-1* polarity defects in VD neurons. Pictures of dorsal synapse morphology after *unc-30* RNAi in wild-type animals, *sad-1* mutants and *sad-1* animals carrying the SAD-1 rescuing construct are shown. (**C**) Quantification of ectopic dorsal-puncta number in animals treated with *unc-30* RNAi (*n*=15, *P*<0.001 all versus wild type). (**D**) Both SAD-1-long (*sad-1+SAD-1(l)*) and -short (*sad-1+SAD-1(s)*) isoform cDNAs expressed from *Punc-25* rescue synapse morphology defects. Morphology of *juIs1* puncta in the dorsal nerve cords of L4-stage animals is shown. (**E**) Only SAD-1-long-isoform cDNA rescued the VD polarity defects of *sad-1* mutation. Pictures of the dorsal synapses in animals carrying the same expression arrays as in D after *unc-30* RNAi. (**F**) Quantification of ectopic dorsal synapse number by VD neurons of animals treated with *unc-30* RNAi in E (*n*=15, *P*<0.001 versus wild type). Scale bar: 5 μm in A,D.

required for neuronal polarity only, allowing a mechanistic separation of different pathways through which SAD-1 regulates the development of the nervous system.

SAD-1 regulates neuronal polarity

Consistent with a role of SAD-A and SAD-B in regulating neuronal polarity, our previous and current studies also determine that SAD-1 is required for establishing axon-dendrite polarity in a variety of *C. elegans* neurons. The role of SAD-family kinases in regulating neuronal polarities is thus evolutionarily conserved. A previous study has shown that the overexpression of SAD-1 also induced neuronal polarity defects in the chemosensory ASI neurons in *C. elegans* (Crump et al., 2001). In this present study, we also noticed synaptic defects induced by high levels of overexpression of SAD-1 (our unpublished observations). Therefore, SAD-1 level is also crucial for proper synapse formation and neuronal-polarity establishment.

NAB-1 provides specificity to SAD-1 function

The interaction with NAB-1 is required for the role of SAD-1 in neuronal polarization, but is completely dispensable for synapse morphology. NAB-1 may allow the specific activation of SAD-1 kinase by restricting SAD-1 to specific compartments in developing neurites. It could also facilitate the functional specificity of SAD-1 by recruiting SAD-1 regulators or substrates specific for neuronal polarity through its protein-interacting modules. Although our studies demonstrated that NAB-1 and SAD-1 co-localize at presynaptic termini, NAB-1 and SAD-1 do not appear to be required for the subcellular localization of one another. We did not observe obvious subcellular mis-localization of NAB-1::GFP in *sad-1* mutants, or vice versa (data not shown). It remains possible that NAB-1 localizes SAD-1 transiently during early neurite outgrowth or that the interaction further refines the localization of these proteins at subdomains of presynaptic termini, because both SAD-1::mRFP and NAB-1::GFP appeared more punctate when co-expressed (Fig. 5F). However, our ability to detect these potential changes is currently limited by a very narrow time window for axon growth and the extremely small size of synapses.

Besides spatially restricting components of signaling pathways and recruiting their regulators and substrates, some scaffolding proteins mediate the cross-talk between signaling pathways. For example, Paxillin, a scaffold for the Raf-1-MEK-ERK MAPK cascade, can recruit and regulate the activation of the focal adhesion kinase, and subsequently Rac, to mediate cell migration (Ishibe et al., 2004; Ishibe et al., 2003). NAB-1 may function in a similar fashion to recruit SAD-1 to a signaling complex that regulates neuronal polarity. Identification of physiological binding partners of NAB-1 will help determine targets, regulators and the signaling pathways through which SAD-1 regulates polarity.

A Neurabin-family protein regulates neuronal polarity

Studies of mammalian Neurabins have focused on the maturation and motility of dendritic spines. In cultured neurons, the F-actin-binding domain is required to promote dendritic-spine maturation (Terry-Lorenzo et al., 2005; Zito et al., 2004). Consistently, both Neurabin- and Spinophilin-knockout mice displayed defects in synaptic plasticity (Allen et al., 2006; Feng et al., 2000; Stafstrom-Davis et al., 2001). Interestingly, invertebrate Neurabins are highly conserved with their mammalian homologs in all other motifs, with the exception of the F-actin-binding domain. Whereas *C. elegans* neurons have no dendritic spines, at least some *Drosophila* neurons show dendritic-spine-like structures that are enriched for actins (Scott et al., 2003). Our studies showed that the *C. elegans* NAB-1 protein controls axon-dendrite determination in a variety of neurons, and that this physiological role depends only on the conserved protein domains between the vertebrate and invertebrate Neurabins. This suggests a potentially conserved role for the Neurabin-protein family during early neurite differentiation. It is possible that mammalian Neurabins play roles prior to dendritic-spine maturation, because blocking their expression inhibits neurite outgrowth in cultured neurons (Nakanishi et al., 1997; Orioli et al., 2006).

Overlapping and non-overlapping roles of SAD-1 and NAB-1

The genetic interactions between *sad-1* and *nab-1* indicate that they function in the same pathway to regulate neuronal polarity. This functional overlap is absent in the regulation of synapse morphology; therefore, SAD-1 regulates synapse morphology through currently unknown mechanisms independent of NAB-1.

In addition to the difference in their requirement for synapse morphology, *sad-1* and *nab-1* mutants display some differences in the severity of their polarity phenotypes. In both *sad-1* and *nab-1* mutants, GABAergic and cholinergic motoneurons accumulate ectopic synaptic vesicles in dendrites, and the number of normal synapses is reduced, which could be secondary to the polarity deficits. In VD neurons, the total number of synapses in *sad-1* mutants is very slightly reduced; by contrast, *nab-1* mutants display a much larger decrease in synapse number. Moreover, the severity of the polarity defects differs slightly in different neurons of *nab-1* and *sad-1* mutants. While the penetrance and number of dendritic vesicle clusters in DD and VD neurons are comparable in *sad-1* and *nab-1* mutants, in ASI and DA neurons, *nab-1* mutants display a much higher penetrance of dendritic synaptic-vesicle clusters than in *sad-1* mutants. This variability suggests that NAB-1 modulates neuron polarity through SAD-1 as well as through other regulators, and that the level of dependence of NAB-1 function on SAD-1 varies in different neurons.

Different genetic pathways regulating neuronal polarity

Previous studies have identified few genes that regulate neuronal polarity in *C. elegans*. SYD-1, a protein with PDZ and Rho-GAP domains, also restricts presynaptic proteins in DD and VD motoneurons (Hallam et al., 2002). Similar to *nab-1* and *sad-1*, disruption of the *syd-1* gene does not lead to lethality or severe locomotion paralysis (Hallam et al., 2002). The genetic interactions between *sad-1*, *nab-1* and *syd-1* are most consistent with SYD-1 functioning either in parallel with, or independently of, NAB-1 and SAD-1, because *syd-1* mutations further enhance the VD polarity defects in both *sad-1* and *nab-1* mutants. *syd-1* mutants also display different phenotypes in DD neurons, which have normal synapse number after the L1 stage in these mutants (Hallam et al., 2002), whereas both *nab-1* and *sad-1* mutants have a decrease in synapse number (Fig. 1B).

These interactions suggest that multiple genetic pathways regulate neuronal polarity in *C. elegans*. Our biochemical and genetic analyses have defined two components of one novel signaling pathway through which the interaction between NAB-1 and SAD kinase specifically mediates the restriction of axon fate in neurite differentiation.

References

Allen, P. B., Ouimet, C. C. and Greengard, P. (1997). Spinophilin, a novel protein phosphatase 1 binding protein localized to dendritic spines. *Proc. Natl. Acad. Sci. USA* **94**, 9956-9961.

Allen, P. B., Zachariou, V., Svenningsson, P., Lepore, A. C., Centonze, D., Costa, C., Rossi, S., Bender, G., Chen, G., Feng, J. et al. (2006). Distinct roles for spinophilin and neurabin in dopamine-mediated plasticity. *Neuroscience* **140**, 897-911.

Arimura, N. and Kaibuchi, K. (2005). Key regulators in neuronal polarity. *Neuron* **48**, 881-884.

Baas, P. W., Black, M. M. and Banker, G. A. (1989). Changes in microtubule polarity orientation during the development of hippocampal neurons in culture. *J. Cell Biol.* **109**, 3085-3094.

Biernat, J., Wu, Y. Z., Timm, T., Zheng-Fischhofer, Q., Mandelkow, E., Meijer, L. and Mandelkow, E. M. (2002). Protein kinase MARK/PAR-1 is required for neurite outgrowth and establishment of neuronal polarity. *Mol. Biol. Cell* **13**, 4013-4028.

Bouquet, C., Soares, S., von Boxberg, Y., Ravaille-Veron, M., Propst, F. and Nothias, F. (2004). Microtubule-associated protein 1B controls directionality of growth cone migration and axonal branching in regeneration of adult dorsal root ganglia neurons. *J. Neurosci.* **24**, 7204-7213.

Buchsbaum, R. J., Connolly, B. A. and Feig, L. A. (2003). Regulation of p70 S6 kinase by complex formation between the Rac guanine nucleotide exchange factor (Rac-GEF) Tiam1 and the scaffold spinophilin. *J. Biol. Chem.* **278**, 18833-18841.

Burnett, P. E., Blackshaw, S., Lai, M. M., Qureshi, I. A., Burnett, A. F., Sabatini, D. M. and Snyder, S. H. (1998). Neurabin is a synaptic protein linking p70 S6 kinase and the neuronal cytoskeleton. *Proc. Natl. Acad. Sci. USA* **95**, 8351-8356.

Chen, X. and Macara, I. G. (2005). Par-3 controls tight junction assembly through the Rac exchange factor Tiam1. *Nat. Cell Biol.* **7**, 262-269.

Crump, J. G., Zhen, M., Jin, Y. and Bargmann, C. I. (2001). The SAD-1 kinase regulates presynaptic vesicle clustering and axon termination. *Neuron* **29**, 115-129.

Dotti, C. G., Sullivan, C. A. and Banker, G. A. (1988). The establishment of polarity by hippocampal neurons in culture. *J. Neurosci.* **8**, 1454-1468.

Eastman, C., Horvitz, H. R. and Jin, Y. (1999). Coordinated transcriptional regulation of the *unc-25* glutamic acid decarboxylase and the *unc-47* GABA vesicular transporter by the *Caenorhabditis elegans* UNC-30 homeodomain protein. *J. Neurosci.* **19**, 6225-6234.

Etienne-Manneville, S. and Hall, A. (2001). Integrin-mediated activation of Cdc42 controls cell polarity in migrating astrocytes through PKCzeta. *Cell* **106**, 489-498.

Feng, J., Yan, Z., Ferreira, A., Tomizawa, K., Liauw, J. A., Zhuo, M., Allen, P. B., Ouimet, C. C. and Greengard, P. (2000). Spinophilin regulates the formation and function of dendritic spines. *Proc. Natl. Acad. Sci. USA* **97**, 9287-9292.

Fire, A., Xu, S., Montgomery, M. K., Kostas, S. A., Driver, S. E. and Mello, C. C. (1998). Potent and specific genetic interference by double-stranded RNA in *Caenorhabditis elegans*. *Nature* **391**, 806-811.

Goold, R. G. and Gordon-Weeks, P. R. (2005). The MAP kinase pathway is upstream of the activation of GSK3β that enables it to phosphorylate MAP1B and contributes to the stimulation of axon growth. *Mol. Cell. Neurosci.* **28**, 524-534.

Hallam, S. J. and Jin, Y. (1998). *lin-14* regulates the timing of synaptic remodelling in *Caenorhabditis elegans*. *Nature* **395**, 78-82.

Hallam, S. J., Goncharov, A., McEwen, J., Baran, R. and Jin, Y. (2002). SYD-1, a presynaptic protein with PDZ, C2 and rhoGAP-like domains, specifies axon identity in *C. elegans*. *Nat. Neurosci.* **5**, 1137-1146.

Hilliard, M. A. and Bargmann, C. I. (2006). Wnt signals and frizzled activity orient anterior-posterior axon outgrowth in *C. elegans*. *Dev. Cell* **10**, 379-390.

Horvitz, H. R., Sternberg, P. W., Greenwald, I. S., Fixsen, W. and Ellis, H. M. (1983). Mutations that affect neural cell lineages and cell fates during the development of the nematode *Caenorhabditis elegans*. *Cold Spring Harb. Symp. Quant. Biol.* **48**, 453-463.

Inoue, E., Mochida, S., Takagi, H., Higa, S., Deguchi-Tawarada, M., Takao-Rikitsu, E., Inoue, M., Yao, I., Takeuchi, K., Kitajima, I. et al. (2006). SAD: a

presynaptic kinase associated with synaptic vesicles and the active zone cytomatrix that regulates neurotransmitter release. *Neuron* **50**, 261-275.

Ishibe, S., Joly, D., Zhu, X. and Cantley, L. G. (2003). Phosphorylation-dependent paxillin-ERK association mediates hepatocyte growth factor-stimulated epithelial morphogenesis. *Mol. Cell* **12**, 1275-1285.

Ishibe, S., Joly, D., Liu, Z. X. and Cantley, L. G. (2004). Paxillin serves as an ERK-regulated scaffold for coordinating FAK and Rac activation in epithelial morphogenesis. *Mol. Cell* **16**, 257-267.

Kempf, M., Clement, A., Faissner, A., Lee, G. and Brandt, R. (1996). Tau binds to the distal axon early in development of polarity in a microtubule- and microfilament-dependent manner. *J. Neurosci.* **16**, 5583-5592.

Kishi, M., Pan, Y. A., Crump, J. G. and Sanes, J. R. (2005). Mammalian SAD kinases are required for neuronal polarization. *Science* **307**, 929-932.

Liao, E. H., Hung, W., Abrams, B. and Zhen, M. (2004). An SCF-like ubiquitin ligase complex that controls presynaptic differentiation. *Nature* **430**, 345-350.

Lorson, M. A., Horvitz, H. R. and van den Heuvel, S. (2000). LIN-5 is a novel component of the spindle apparatus required for chromosome segregation and cleavage plane specification in *Caenorhabditis elegans*. *J. Cell Biol.* **148**, 73-86.

Menager, C., Arimura, N., Fukata, Y. and Kaibuchi, K. (2004). PIP3 is involved in neuronal polarization and axon formation. *J. Neurochem.* **89**, 109-118.

Miller, D. M., III and Niemeyer, C. J. (1995). Expression of the *unc-4* homeoprotein in *Caenorhabditis elegans* motor neurons specifies presynaptic input. *Development* **121**, 2877-2886.

Muly, E. C., Allen, P., Mazloom, M., Aranbayeva, Z., Greenfield, A. T. and Greengard, P. (2004a). Subcellular distribution of neurabin immunolabeling in primate prefrontal cortex: comparison with spinophilin. *Cereb. Cortex* **14**, 1398-1407.

Muly, E. C., Smith, Y., Allen, P. and Greengard, P. (2004b). Subcellular distribution of spinophilin immunolabeling in primate prefrontal cortex: localization at and within dendritic spines. *J. Comp. Neurol.* **469**, 185-197.

Nakamura, Y., Makabe, K. W. and Nishida, H. (2005). POPK-1/Sad-1 kinase is required for the proper translocation of maternal mRNAs and putative germ plasm at the posterior pole of the ascidian embryo. *Development* **132**, 4731-4742.

Nakanishi, H., Obaishi, H., Satoh, A., Wada, M., Mandai, K., Satoh, K., Nishioka, H., Matsuura, Y., Mizoguchi, A. and Takai, Y. (1997). Neurabin: a novel neural tissue-specific actin filament-binding protein involved in neurite formation. *J. Cell Biol.* **139**, 951-961.

Nishimura, T., Yamaguchi, T., Kato, K., Yoshizawa, M., Nabeshima, Y., Ohno, S., Hoshino, M. and Kaibuchi, K. (2005). PAR-6-PAR-3 mediates Cdc42-induced Rac activation through the Rac GEFs STEF/Tiam1. *Nat. Cell Biol.* **7**, 270-277.

Orioli, D., Colaluca, I. N., Stefanini, M., Riva, S., Dotti, C. G. and Peverali, F. A. (2006). Rac3-induced neuritogenesis requires binding to Neurabin I. *Mol. Biol. Cell* **17**, 2391-2400.

Pan, C. L., Howell, J. E., Clark, S. G., Hilliard, M., Cordes, S., Bargmann, C. I. and Garriga, G. (2006). Multiple Wnts and frizzled receptors regulate anteriorly directed cell and growth cone migrations in *Caenorhabditis elegans*. *Dev. Cell* **10**, 367-377.

Prasad, B. C. and Clark, S. G. (2006). Wnt signaling establishes anteroposterior neuronal polarity and requires retromer in *C. elegans*. *Development* **133**, 1757-1766.

Richman, J. G., Brady, A. E., Wang, Q., Hensel, J. L., Colbran, R. J. and Limbird, L. E. (2001). Agonist-regulated Interaction between α2-adrenergic receptors and spinophilin. *J. Biol. Chem.* **276**, 15003-15008.

Rolls, M. M. and Doe, C. Q. (2004). Baz, Par-6 and aPKC are not required for axon or dendrite specification in *Drosophila*. *Nat. Neurosci.* **7**, 1293-1295.

Ryan, X. P., Alldritt, J., Svenningsson, P., Allen, P. B., Wu, G. Y., Nairn, A. C. and Greengard, P. (2005). The Rho-specific GEF Lfc interacts with neurabin and spinophilin to regulate dendritic spine morphology. *Neuron* **47**, 85-100.

Satoh, A., Nakanishi, H., Obaishi, H., Wada, M., Takahashi, K., Satoh, K., Hirao, K., Nishioka, H., Hata, Y., Mizoguchi, A. et al. (1998). Neurabin-II/spinophilin. An actin filament-binding protein with one PDZ domain localized at cadherin-based cell-cell adhesion sites. *J. Biol. Chem.* **273**, 3470-3475.

Scott, E. K., Reuter, J. E. and Luo, L. (2003). Small GTPase Cdc42 is required for multiple aspects of dendritic morphogenesis. *J. Neurosci.* **23**, 3118-3123.

Shi, S. H., Jan, L. Y. and Jan, Y. N. (2003). Hippocampal neuronal polarity specified by spatially localized mPar3/mPar6 and PI 3-kinase activity. *Cell* **112**, 63-75.

Smith, F. D., Oxford, G. S. and Milgram, S. L. (1999). Association of the D2 dopamine receptor third cytoplasmic loop with spinophilin, a protein phosphatase-1-interacting protein. *J. Biol. Chem.* **274**, 19894-19900.

Stafstrom-Davis, C. A., Ouimet, C. C., Feng, J., Allen, P. B., Greengard, P. and Houpt, T. A. (2001). Impaired conditioned taste aversion learning in spinophilin knockout mice. *Learn. Mem.* **8**, 272-278.

Terry-Lorenzo, R. T., Carmody, L. C., Voltz, J. W., Connor, J. H., Li, S., Smith, F. D., Milgram, S. L., Colbran, R. J. and Shenolikar, S. (2002a). The neuronal

actin-binding proteins, neurabin I and neurabin II, recruit specific isoforms of protein phosphatase-1 catalytic subunits. *J. Biol. Chem.* **277**, 27716-27724.

Terry-Lorenzo, R. T., Elliot, E., Weiser, D. C., Prickett, T. D., Brautigan, D. L. and Shenolikar, S. (2002b). Neurabins recruit protein phosphatase-1 and inhibitor-2 to the actin cytoskeleton. *J. Biol. Chem.* **277**, 46535-46543.

Terry-Lorenzo, R. T., Roadcap, D. W., Otsuka, T., Blanpied, T. A., Zamorano, P. L., Garner, C. C., Shenolikar, S. and Ehlers, M. D. (2005). Neurabin/protein phosphatase-1 complex regulates dendritic spine morphogenesis and maturation. *Mol. Biol. Cell* **16**, 2349-2362.

Trivedi, N., Marsh, P., Goold, R. G., Wood-Kaczmar, A. and Gordon-Weeks, P. R. (2005). Glycogen synthase kinase-3β phosphorylation of MAP1B at Ser1260 and Thr1265 is spatially restricted to growing axons. *J. Cell Sci.* **118**, 993-1005.

Wang, X., Zeng, W., Soyombo, A. A., Tang, W., Ross, E. M., Barnes, A. P., Milgram, S. L., Penninger, J. M., Allen, P. B., Greengard, P. et al. (2005). Spinophilin regulates Ca2+ signalling by binding the N-terminal domain of RGS2

and the third intracellular loop of G-protein-coupled receptors. *Nat. Cell Biol.* **7**, 405-411.

White, J. G., Albertson, D. G. and Anness, M. A. (1978). Connectivity changes in a class of motoneurone during the development of a nematode. *Nature* **271**, 764-766.

White, J. G., Southgate, E., Thomson, J. N. and Brenner, S. (1986). The structure of the nervous system of the nematode *Caenorhabditis elegans*. *Philos. Trans. R. Soc. Lond. B Biol. Sci.* **314**, 1-340.

Wiggin, G. R., Fawcett, J. P. and Pawson, T. (2005). Polarity proteins in axon specification and synaptogenesis. *Dev. Cell* **8**, 803-816.

Yeh, E., Kawano, T., Weimer, R. M., Bessereau, J. L. and Zhen, M. (2005). Identification of genes involved in synaptogenesis using a fluorescent active zone marker in *Caenorhabditis elegans*. *J. Neurosci.* **25**, 3833-3841.

Zito, K., Knott, G., Shepherd, G. M., Shenolikar, S. and Svoboda, K. (2004). Induction of spine growth and synapse formation by regulation of the spine actin cytoskeleton. *Neuron* **44**, 321-334.

DEVELOPMENT